Removal of Arsenic from Aqueous Solutions Using Zirconium Oxyhydrate Embedded Fe₃O₄ Nanoparticle

SHAOLIN WU[1,2,*], WENTAO HU[1,2] and MING MA[1,2]

[1]Key Laboratory of Jiangxi Province for Ecological Diagnosis-Remediation and Pollution Control, Nanchang 330063, P.R. China
[2]School of Environmental and Chemical Engineering, Nanchang Hangkong University, Nanchang 330063, P.R. China

*Corresponding author: Fax: +86 791 395373; Tel: +86 791 3953372; E-mail: hupeng_521@yahoo.com.cn

A new type of magnetic nanoparticle $Fe_3O_4@ZrO(OH)_2$ was prepared in Fe_3O_4 coated with zirconium oxyhydrate in order to remove high concentration toxic substances *i.e.*, As(III/V) from aqueous solutions. This magnetic nanoparticle contained high attractive toward arsenic because zirconium oxyhydrate and excellent magnetic separability in the high-intensity magnetic field as well as good repeated for many times. The major effects on the removal of As(III/V), such as initial As(III/V) concentration, adsorption time, temperature, solution pH, co-existing anions, deabsorption and removal efficiency were investigated. The results clearly showed that the maximum adsorption capacity of $Fe_3O_4@ZrO(OH)_2$ to As(III) and As(V) calculated by Langmuir equation were 188.68 and 108.70 mg/g, respectively. The adsorption time effect followed a pseudo-second-order rate equation, can get contact time to As(III/V) of 20 min to reach equilibrium. The enthalpy change (ΔH°) and entropy change (ΔS°) of As(III) were 17.38, 61.43 J/mol/K, which indicates the spontaneous nature of the As(III) adsorption process. The adsorption capacity of As(III) was increased from solution pH were 2-6 and decreased when pH were 9-12, while As(V) was always decreased along with the increase of solution pH. Interference ions have more effect As(III) than As(V). This magnetic nanoparticle could use more than four times after it was desorbed by NaOH. Besides, after using $Fe_3O_4@ZrO(OH)_2$ as adsorbent to deal with an initial concentration of 10 mg/L of As(III) and 1 mg/L of As(V) solution, surplus concentration of arsenic less than 10 ppb. It is concluded that the magnetic nanoparticle $Fe_3O_4@ZrO(OH)_2$ can be considered as a good settlement performance, high arsenic uptake capability and fine utilization make it potentially excellent and attractive material for arsenic removal in future.

Key Words: Arsenate, Arsenite, Adsorption, Fe₃O₄@ZrO(OH)₂.

INTRODUCTION

Arsenic is one of the toxic and carcinogenic substance in the drinking water is presently of a worldwide concern. The toxicity of arsenic to humans is well documented, which leads to some organs canceration including skin, lung, liver, kidney and bladder cancers[1,2]. Arsenic pollution due to natural factors and anthropogenic activities has been reported in a large amount of regions, especially in Asian countries, such us China, New Zealand, Japan and India[3]. In view of this, the World Health Organization (WHO) has set a maximum permissible concentration for arsenic in drinking water at 10 µg/L in 1993[4,5]. Consequently, removal of arsenic form drinking water is an imperative work of people's livelihood and our world.

Several effective technologies have been employed for removal of both As(III) and As(V) species in aqueous solution over the last few decades, including precipitation[6,7], ion-exchange[8], electrochemical measurement[9], biotechno-logy[10], membrane filtration[11] and adsorption[12-14]. Nevertheless,

the difficulties to eliminate impurities of coagulation techno-logy, high cost of resins and membrane, long period of the biotechnology are restricting their development. In order to develop such remediation technologies, adsorption is regarded as a potential method for its innovative attraction and economy. One of the standards for the selection of adsorbent mainly depends on its economic benefit and adsorption capacity. In recent years, a wide range of reasonable price sorbent materials such as zero-valent iron[15], iron-containing compounds[16,17], aluminum salt[18], thulium, clay[19], modified matter[20], combi-nation substance[21], active material[22], have been tested for removing arsenic from drinking water. However, the low adsorption capacities and slow adsorption speed of those materials are insufficient for wide application. As a novel adsorption material, nanoparticles[23] are applied broadly owing to its outstanding adsorption capacity. Whereas its high cost, low reuse times and low recovery efficiency have limited its application in drinking water, particularly in the developing world. In order to overcome these drawbacks of the adsorbents,

we picked the magnetic nanoparticle $Fe_3O_4@ZrO(OH)_2$ prepared in Fe_3O_4 coated with zirconium oxyhydrate because of transition metal zirconium own natural and excellent adsorption ability for arsenic solution and nanoparticles of Fe_3O_4 owing its high surface area and good magnetic separability.

In this present work, on the basis of chemical coprecipitation method we smoothly used zirconium oxyhydrate embedded with Fe_3O_4 nanoparticle synthesized magnetic nanoparticles as $Fe_3O_4@ZrO(OH)_2$. It has high surface area for nanoparticles and excellent adsorption ability for hydrogen zirconium oxide attached to the Fe_3O_4 surface. Moreover, it possesses strong magnetic properties could easily achieve solid-liquid separation through an external magnetic field. To our surprise, these magnetic nanoparticles adsorbent can be reused more than four times after desorbtion. Furthermore we investigated the adsorption behaviour including adsorption isotherm, adsorption kinetics, solution pH, co-existing anions, desorption and removal efficiency of $Fe_3O_4@ZrO(OH)_2$ to As(III) and As(V).

EXPERIMENTAL

All reagents used in the experiment were analytical reagent-grade except HCl (GR). $FeCl_3·6H_2O$, $FeSO_4·7H_2O$ were purchased from Xilong Chemical Corporation (Shantou, China) $ZrOCl_2·8H_2O$ was bought from sinohparm chemical reagent Corporation (shanghai, China). $Na_2HAsO_4·12H_2O$ (AR) and $NaAsO_2$ (AR) obtained from Beijing Chemicals Corporation (Beijing, China). Ultrapure water used in all of the experiments was prepared by using Milli-Q water purification system (Xiamen China).

Preparation of magnetic nanoparticles $Fe_3O_4@ZrO(OH)_2$: In order to prepare $Fe_3O_4@ZrO(OH)_2$, Fe_3O_4 was synthesized first of all. The Fe_3O_4 magnetic nanoparticles were prepared by the chemical coprecipitation method. The optimum experimental conditions for synthesizing Fe_3O_4 with appreciable modification as follows[24]: 27.029 g of $FeCl_3·6H_2O$ and 13.901 g of $FeSO_4·7H_2O$ were mixed in three-neck flask in 50 mL ultrapure water, degassed with N_2 2-3 min. Then the mixed solution was stirred and heated (85 ℃) in thermostat water bath cauldron. When the temperature of the mixture was stable, 2.0 M NaOH was dropwise added to three-neck flask. Stop dropping when the solution into bright black. Fe_3O_4 nanoparticles were synthesized 2 h later. It was collected by a magnet and rinsed with deionized water for two times. Resuspended in 200 mL ultrapure water after washing.

10 mL Fe_3O_4 nanoparticles suspending liquid were mixed 0.01 M, 100 mL $ZrOCl_2·8H_2O$ in three-neck flask. Then 2.0 M NaOH was dropwise added to three-neck flask. Stop dropping when the solution into bright black. After 2 h, collected by a magnet and washed until the pH of the supernatant reached *ca.* 7. Resuspended in 200 mL ultrapure water preserve it by sealing it airtight after washing. This is $Fe_3O_4@ZrO(OH)_2$. During the whole process, temperature was maintained at 85 ℃ and solution was stirred. Now the mass ratio of Fe_3O_4-$ZrOCl_2·8H_2O$ was 5:3. Similarly, displacement 20-30 mL Fe_3O_4 nanoparticles suspending liquid. Synthesized $Fe_3O_4@ZrO(OH)_2$ in which the mass ratio of Fe_3O_4-$ZrOCl_2·8H_2O$ was 10:3, 15:3.

Preparation of arsenite [As(III)] and arsenate [As(V)] standard solutions: The As(III/V) stock solution (concentration of 1 g/L) was prepared from 0.1734 g of $NaAsO_2$ and 0.537 g of $Na_2HAsO_4·12H_2O$ dissolved in H_2SO_4 (1 %) to volumetric flask (100 mL), respectively. Obtain every different concentration ready for the continuation use through dilution effect. The pH of the solutions was adjusted with HCl and NaOH to designated values in the range of 2-12.

Arsenic adsorption: Batch adsorption experiments were conducted by adding 20 mL aqueous solution in 100 mL conical flask. Solution pH was adjusted with HCl and NaOH to designated values. The $Fe_3O_4@ZrO(OH)_2$ suspensions were stirred and ultrasonic washing 10 min. Then 1 mL of $Fe_3O_4@ZrO(OH)_2$ suspensions (10 mg/mL) was added into conical flask. The mixtures were shaken for 0.5 h in constant temperature oscillation box at 25 ℃. The supernatant were collected use a strong magnet bar was placed on the bottom of the conical flask. Then the residual concentrations of arsenic were determined with an AFS-8220.

The isotherm tests were carried out with a series of initial arsenic concentrations reach to the equilibrium. The solution pH and temperature was controlled at 6-7 and 25 ℃, respectively. The kinetic experiments were conducted by the time-dependent adsorption reactions. Different initial arsenic concentrations and different temperature were investigated. The tests of all kinds of anions and water adsorption indicate that various anions co-exist with arsenic effects the adsorption capacity of arsenic. The desorption tests were carried out using NaOH elution the $Fe_3O_4@ZrO(OH)_2$ were adsorbed in order to obtain the desorption times of $Fe_3O_4@ZrO(OH)_2$.

Analytic method: The atomic fluorescence spectrometry (AFS-8220) was used to determine the arsenic. This instrument was equipped with a boosted-discharge hollow cathode lamp, the separation of the gaseous arsines from the liquid stream was performed in a PS analytical type A gas-liquid separator, using argon as carrier gas. A hydrogen flow was also added to support the hydrogen-argon diffusion flame of the detector. The analog signal output was connected to a computer[25].

RESULTS AND DISCUSSION

Adsorption isotherms: Langmuir and Freundlich isotherm models were used to analyze the experimental adsorption equilibrium date. It is presented by the following equation[26]:

$$\frac{C_e}{q_e} = \frac{C_e}{q_m} + \frac{1}{k_L q_m} \tag{1}$$

$$\log q_e = \frac{1}{n}\log C_e + \log k_F \tag{2}$$

where q_e (mg/g) and C_e (mg/L) were the equilibrium adsorption capacity and the equilibrium adsorbate concentration, respectively; K_L (L/mg) and q_m (mg/g) are the Langmuir constants related to the energy of adsorption and maximum capacity, respectively; K_F ($mg^{1-(1/n)}L^{1/n}/g$) and $1/n$ are the Freundlich constants related to the adsorption capacity and intensity, respectively.

The equilibrium data for As(III) and As(V) adsorption are shown in Fig. 1. The magnetic $Fe_3O_4@ZrO(OH)_2$ adsorbents possess high affinity to As(III) than As(V) (Fig. 1). With the decreasing mass ratio of $ZrOCl_2·8H_2O$, the amount

of adsorbed As(III/V) decreased distinctly. So the conclusion can be concluded that the $ZrOCl_2 \cdot 8H_2O$ layer thickness results in the adsorption capacity of the $Fe_3O_4@ZrO(OH)_2$.
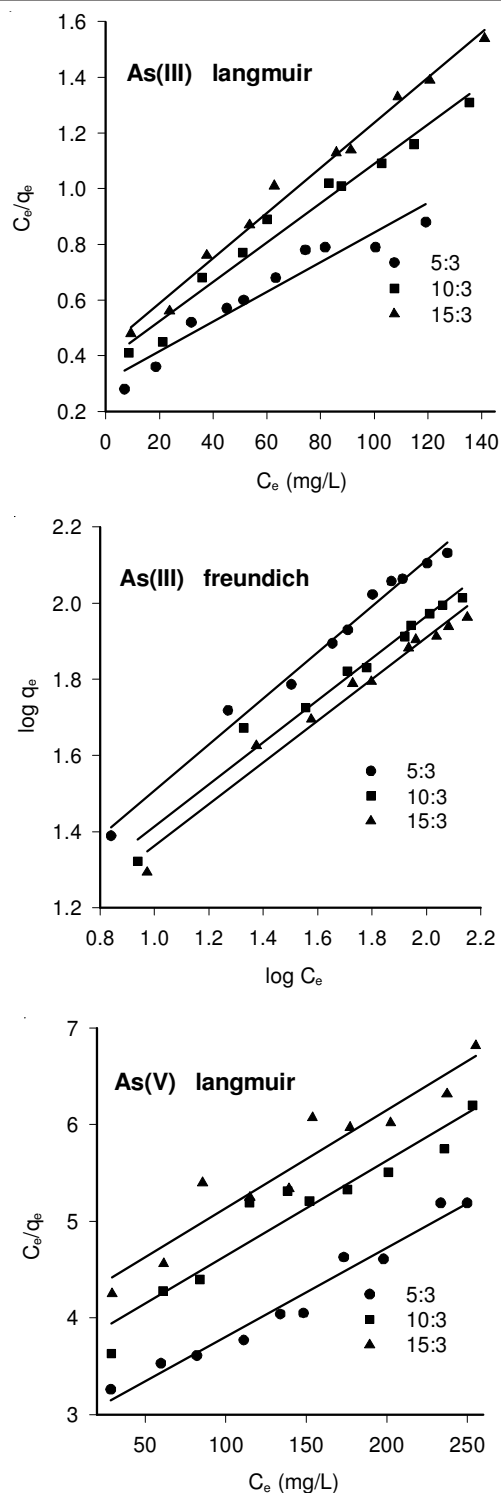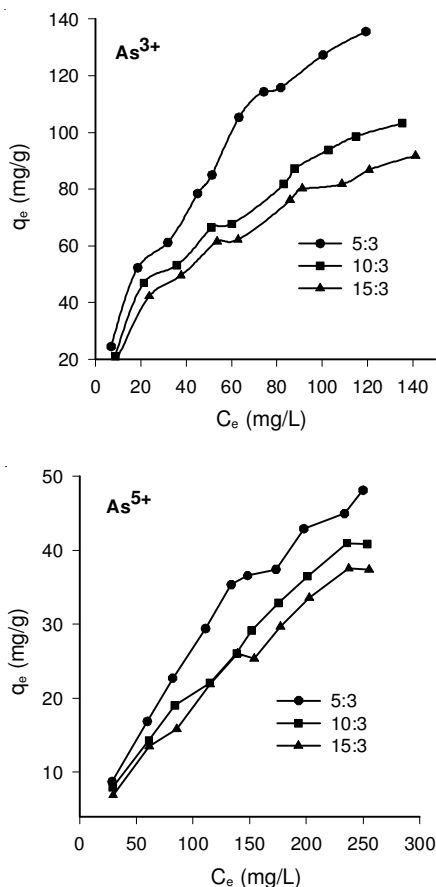
Fig. 1. Adsorption isotherms of As(III) and As(V) by $Fe_3O_4@ZrO(OH)_2$ with various mass ratio of Fe_3O_4 to $ZrOCl_2 \cdot 8H_2O$, pH = 7

The results of fitting Langmuir and Freundlich equations to isotherm curves are presented in Fig. 2. Correlation coefficients were calculated for both isotherm models in Table-1.

Regression coefficients (r^2) for different conditions were larger than 0.91, demonstrating that both Langmuir and freundlich models were fit for representing the adsorption behaviour of As(III/V) on the magnetic $Fe_3O_4@ZrO(OH)_2$. The maximum adsorption capacities (q_m) of As(III) obtained for $Fe_3O_4@ZrO(OH)_2$ (5:3) was 188.68 mg/g, $Fe_3O_4@ZrO(OH)_2$ (10:3) for 140.85 mg/g and $Fe_3O_4@ZrO(OH)_2$ (15:3) for 123.46 mg/g at 25 ºC. Compared with As(V) obtained for $Fe_3O_4@ZrO(OH)_2$ (5:3) was 108.70 mg/g, $Fe_3O_4@ZrO(OH)_2$

TABLE-1
LANGMUIR, FREUNDLICH ISOTHERMS PARAMETERS FOR As(III) AND As(V)
ADSORPTION ONTO THE $Fe_3O_4@ZrO(OH)_2$ NANOPARTICLES

Parameter $Fe_3O_4@ZrO(OH)_2$		Langmuir isotherm model			Freundich isotherm model		
		q_m (mg/g)	K_L (L/mg)	r^2	K_F ($mg^{1-(1/n)}L^{1/n}$/g)	n	r^2
As(III)	10:3	188.68	0.01716	0.9285	8.0131	1.6540	0.9876
	20:3	140.85	0.01851	0.9720	7.2344	1.8080	0.9735
	30:3	123.46	0.01905	0.9887	6.5298	1.8262	0.9752
As(V)	10:3	108.70	0.003187	0.9661	0.6936	1.2825	0.9869
	20:3	101.01	0.002710	0.9185	0.6051	1.3011	0.9965
	30:3	98.04	0.002477	0.9111	0.4928	1.2639	0.9934

As(III/V) at pH 7, adsorbent: 10 mg/mL, temperature: 25 ºC.

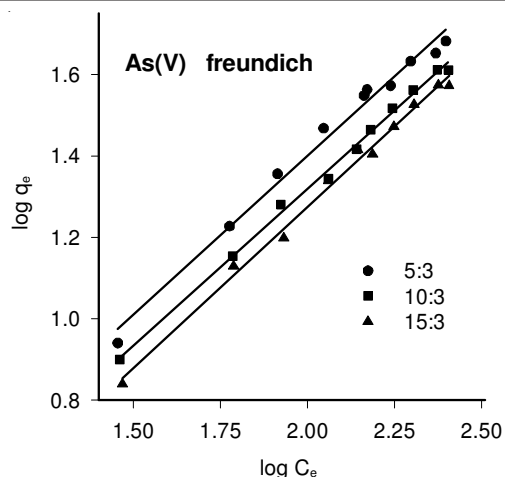Fig. 2. Langmuir, Freundlich isotherms for As(III/V) adsorption on $Fe_3O_4@ZrO(OH)_2$ with various of mass ratio of Fe_3O_4 to $ZrOCl_2\cdot8H_2O$

(10:3) for 101.01 mg/g and $Fe_3O_4@ZrO(OH)_2$ (15:3) for 98.04 mg/g at 25 °C, which was lower than As(III). The Freundlich adsorption intensity parameters (n values) were higher As(III) than As(V) as one reason can account for the adsorption capacity of As(III) is stronger than As(V).

Adsorption kinetics study: Kinetic studies provide information about time required for the establishment of sorption equilibrium. Various models can represent the behaviour of a batch adsorption process. We use the pseudo-second-order kinetic model[26] is presented as:

$$\frac{t}{q_t} = \frac{1}{k_2 q_e^2} + \frac{t}{q_e} \qquad (3)$$

where k_2 is the rate constant of adsorption (g/mg/min), q_t is the amount of arsenic adsorbed by adsorbent at any time (mg/g), q_e is equilibrium adsorption capacity (mg/g) and the initial sorption rate, h_0 (mg/g/min) can be defined as:

$$h_0 = k_2 q_e^2 \; (t \rightarrow o) \qquad (4)$$

Both k_2 and h_0 could be determined experimentally by plotting of t/q_t *versus* t.

The experiments about adsorption rate of As(III/V) adsorption on the $Fe_3O_4@ZrO(OH)_2$ (10:3) nanoparticles surface were carried out by different initial As(III/V) concentration and various chemical reaction temperature. The samples were taken different periods of time and analyzed for their As(III/V) concentration, was shown in Figs. 3 and 4.
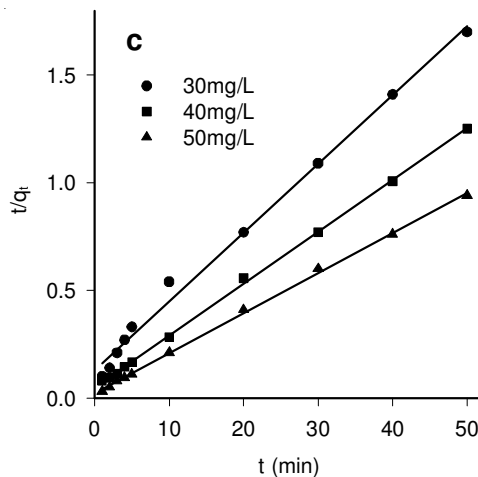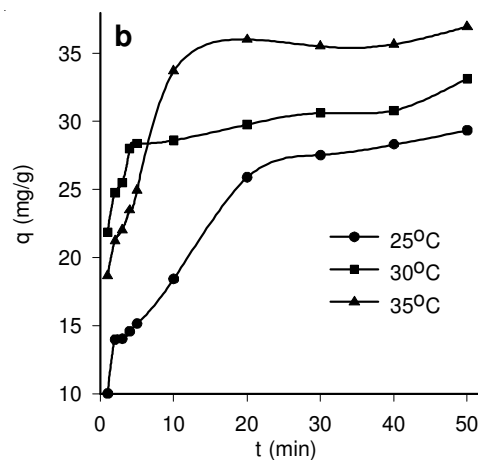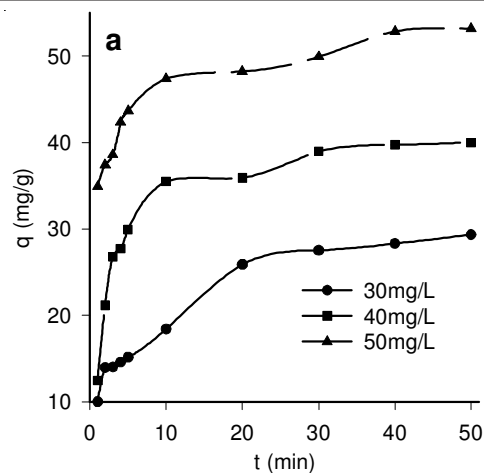
| TABLE-2						
PSEUDO-SECOND-ORDER KINETIC PARAMETERS OF As(III/V) ADSORPTION ONTO THE $Fe_3O_4@ZrO(OH)_2$ (10:3) NANOPARTICLES						
$Fe_3O_4@ZrO(OH)_2$		Different initial concentration[a]			Different temperature[b]		
	Parameter	At 30 mg/L	At 40 mg/L	At 50 mg/L	At 25 °C	At 30 °C	At 35 °C
As (III)	k_2 (g/mg/min)	0.007864	0.01188	0.01663	0.007864	0.03227	0.01447
	q_e (mg/g)	31.35	41.49	53.76	31.35	32.47	38.02
	h_0 (mg/g/min)	7.73	20.45	48.08	7.73	34.01	20.92
	r^2	0.9939	0.9994	0.9989	0.9939	0.9974	0.9988
As (V)	Parameter	At 55 mg/L	At 85 mg/L	At 115 mg/L	At 25 °C	At 30 °C	At 35 °C
	k_2 (g/mg/min)	0.04134	0.01889	0.01568	0.01889	0.01621	0.01158
	q_e (mg/g)	13.66	27.32	39.06	27.32	30.21	33.33
	h_0 (mg/g/min)	7.72	14.10	23.92	14.10	14.79	12.87
	r^2	0.9965	0.9985	0.9997	0.9985	0.9990	0.9970
[a]pH 7, adsorbent: 10 mg/mL, temperature: 25 °C. [b]pH 7, adsorbent: 10 mg/mL, initial As(III/V) concentration: (40/85) mg/L.							
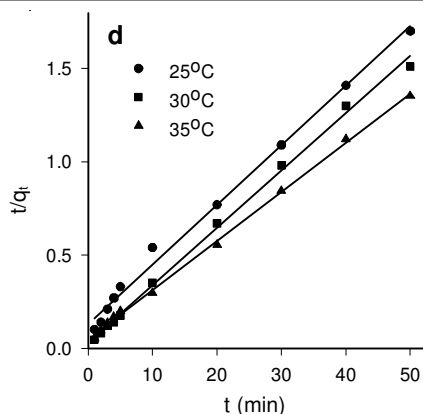
Fig. 3. Effects of reaction time on As(III) removal using adsorbent (a, c) linear fit of experimental data obtained using pseudo-second order kinetic model (b, d). pH = 7; adsorbent:10 mg/mL; temperature: 25 ºC(a); initial As(III) concentration: 40 mg/L (b)
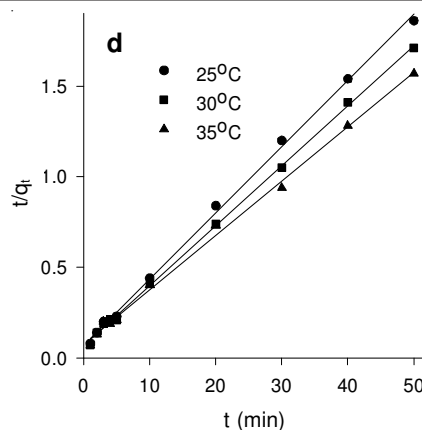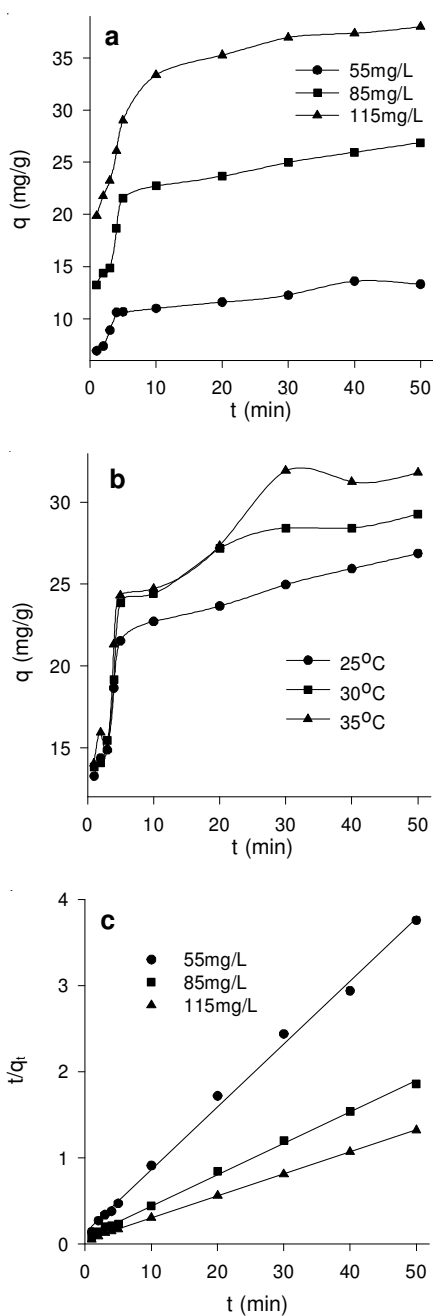

Fig. 4. Effects of reaction time on As(V) removal using adsorbent (a, c) linear fit of experimental data obtained using pseudo-second order kinetic model (b, d). pH = 7; adsorbent: 10 mg/mL; temperature: 25 ºC. (a) Initial As(V) concentration: 85 mg/L (b)

The As(III) removal reached equilibrium after of 20 min can be known from Figs. 3 and 4. However, As(V) could reach to equilibrium about 10 min. Constant k_2 and maximum adsorption capacity q_e were calculated from the intercept and slope of this graph, respectively (Table-2).

The kinetics about magnetic $Fe_3O_4@ZrO(OH)_2$ nanomaterials adsorb As(III) and As(V) are expressed well by pseudo-second-order kinetic model ($r_2 > 0.99$). The initial sorption rate h_0 and equilibrium adsorption capacity q_e values of As(III) were higher than those of As(V), indicating the faster adsorption rate of As(III) than that of As(V). For As(III/V), h_0 and q_e values were higher along with the initial As(III/V) concentration higher.

Thermodynamic parameters: The thermodynamic parameters, the enthalpy change ΔHº and the entropy change ΔSº were calculated from the slope and intercept of the plot of $\log \dfrac{q_e}{C_e}$ against 1/T according to the equation[26]:

$$\log\left(\frac{q_e}{C_e}\right) = \frac{\Delta S^{\circ}}{2.303R} - \left(\frac{\Delta H^{\circ}}{2.303R}\right)\frac{1}{T} \qquad (5)$$

where q_e and C_e are the adsorption equilibrium adsorption capacity and equilibrium concentration, respectively; ΔHº and ΔSº are the change in enthalpy and entropy under standard states, respectively. R is the universal gas constant and T is the Kelvin temperature.

As related to temperature effect, the thermodynamic parameters have been calculated for this adsorption system. The free energy change of adsorption ΔGº is calculated by using the equation:

$$\Delta G^{\circ} = \Delta H^{\circ} - T\Delta S^{\circ} \qquad (6)$$

where ΔGº is the change in free energy.

The adsorption experiments were conducted in the temperature range of 25-35 ºC with $Fe_3O_4@ZrO(OH)_2$ concentration of 10 mg/mL and initial As(III) and As(V) concentration of 30 mg/L and 80mg/L at initial pH 5.0.

ΔHº, ΔGº and Correlation r_2 were obtained by plotting a graph between $\log \dfrac{q_e}{C_e}$ and 1/T as shown in Fig. 5. For
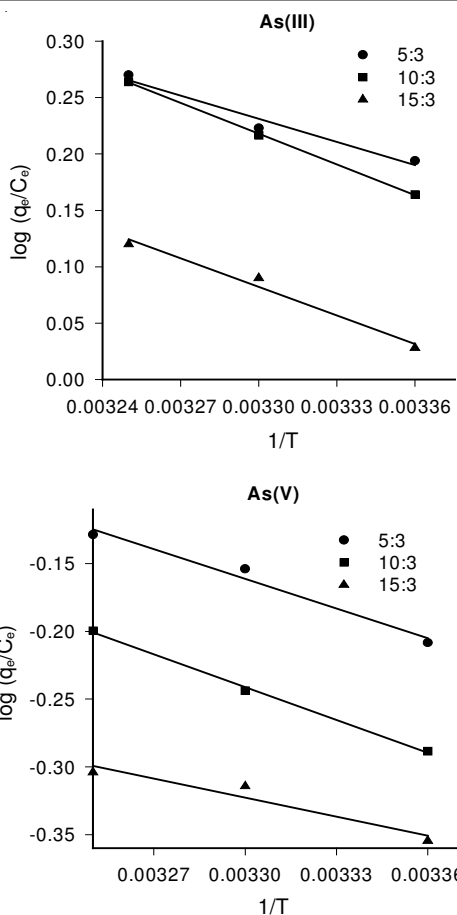
Fig. 5. Thermodynamics equation curve of As(III) and As(V). pH = 7; adsorbent:10 mg/mL; initial As(III/V) concentration:(30/80) mg/L

Fig. 6. Effect of pH on adsorption of As(III) and As(V) on various Fe₃O₄@ZrO(OH)₂ nanoparticles. Adsorbent: 1 mg/mL; temperature: 25 ºC; initial As(III/V) concentration: (50/80) mg/L

example, the calculated value of ΔH° for Fe₃O₄@ZrO(OH)₂(10:3) was 17.38 kJ/mol. The ΔS° was 61.43 J/mol/K. Using the values of ΔH° and ΔS°, the ΔG° values have been calculated by eqn. 6 and shown in Table-3. All of adsorbents of free energy As(III) changed less than zero indicated the adsorption of As(III) spontaneous process, which indicated the spontaneous nature of the As(III) adsorption process.

Effect of pH: The pH of aqueous solution usually plays an important role in deciding the amount of As(III/V) adsorbed on Fe₃O₄@ZrO(OH)₂ nanoparticles[27]. Adsorption experiments were carried out at various aqueous phase pH (2-12) by keeping all other experimental conditions constant(reaction time, 0.5 h; adsorbent concentration,10 mg/L; initial As(III) and As(V) concentration of 50 mg/L and 80 mg/L). 1 mol/L HCl and NaOH concentration were used for adjustment pH. The effect of pH on the adsorbent process was shown in Fig. 6.
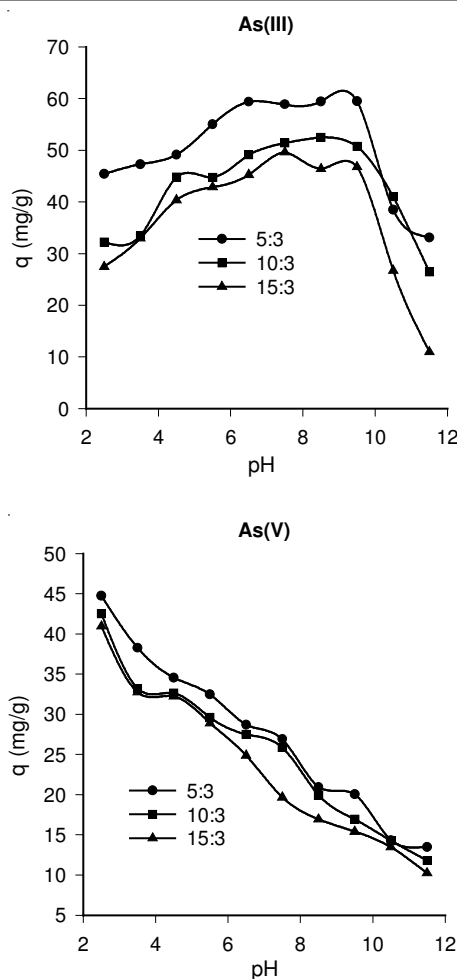
It can be concluded that with the increase of solution pH, adsorption capacity of As(III) on various Fe₃O₄@ZrO(OH)₂ nanoparticles present a certain appearance as parabola from Fig. 6. The adsorption quantity reached the biggest when pH (8-10). However, adsorption capacity of As(V) decreased with the increase of pH on various Fe₃O₄@ZrO(OH)₂ nanoparticles.

Effect of some interference ions over the adsorption capacity of As(III/V): Proverbially, the contaminated drinking and wastewater not only contain arsenic but also include several other co-existing ions, such as nitrate, sulfate and phosphate, which can compete with arsenic ion. When Fe₃O₄@ZrO(OH)₂ nanoparticles adsorb As(III/V). It is considered as the effect of competitive ions on the Fe₃O₄@ZrO(OH)₂.

					ΔG° (kJ mol⁻¹)		
Adsorbent Fe₃O₄@ZrO(OH)₂		ΔH° (kJ mol⁻¹)	ΔS° (J mol⁻¹ K⁻¹)	r²	At 25 ºC	At 30 ºC	At 35 ºC
As(III)	10:3	13.09	47.63	0.9649	-1.104	-1.342	-1.580
	20:3	17.38	61.43	0.9995	-0.9261	-1.233	-1.540
	30:3	16.13	54.80	0.9786	-0.2004	-0.4744	-0.7484
As(V)	10:3	13.98	43.06	0.9756	1.1481	0.9328	0.7175
	20:3	15.44	46.35	0.9975	1.6277	1.396	1.164
	30:3	8.95	23.41	0.9248	1.9738	1.857	1.740

TABLE-3
THERMODYNAMIC PARAMETER FOR ADSORPTION OF As(III/V) ONTO THE Fe₃O₄@ZrO(OH)₂ (10:3) NANOPARTICLES

pH 7; adsorbent: 10 mg/mL; initial As(III/V) concentration: (30/80) mg/L.

Adsorption experiments were carried out by adding 100 mg/L of Cl^-, NO^{3-}, SO_4^{2-}, PO_4^{3-} and tap water, ground water, ganjiang water and ultrapure water preparation for 30 mg/L of As(III) and 80 mg/L of As(V) solution 20 mL throw 2 mL $Fe_3O_4@ZrO(OH)_2$ (10:3). Fig. 8 shows the effect of various co-existing ions and different water environment on As(III/V) adsorption by $Fe_3O_4@ZrO(OH)_2$(10:3).

As can be seen in Fig. 7, most of anion adsorbing capacity of As(III) is less than no ion (ultrapure water) except Ganjiang River. And for As(V), all of the anion adsorbing capacity is more than no ion. Interference ions effect more As(III) than As(V) in spite of the impact of adsorbing capacity is not significant.
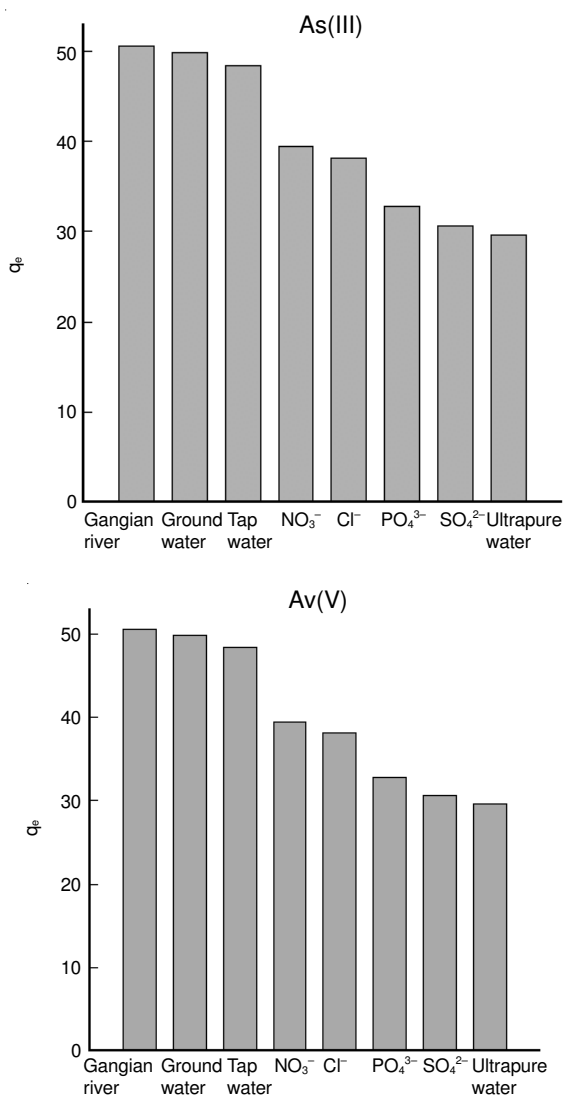

As(III)

As(V)

Fig. 7. Effect of different interference ion on the adsorption of As(III/V) by adsorbent. pH = 7; adsorbent: 1 mg/mL; temperature: 25 °C; initial As(III/V) concentration: (30/80) mg/L

Desorption study: The sorbents has to be amenable to efficient regeneration and reuse. It is important to research the feasibility of $Fe_3O_4@ZrO(OH)_2$ magnetic nanomaterials to be regenerated after adsorption of arsenic. In high pH, the surface hydroxyl groups got deprotonated and negatively charged, resulting in efficiently desorption of negatively charged arsenic species[28]. Desorption study was carried out with

$Fe_3O_4@ZrO(OH)_2$ (10:3) adsorbents conduct 50 mg/L of As(III/V). Put the saturated adsorbent immerse in 2 M NaOH solution at constant temperature oscillation box 20 min with ultrasonic cleaning 10 min for twice, respectively. Then use deionized water to clean the adsorbent until the pH of the supernatant reached *ca.* 7. Fig. 8 showed the adsorption capacity about $Fe_3O_4@ZrO(OH)_2$(10:3) adsorbents for As(III/V) were hardly any change after desorption of arsenic four times. So these magnetic nanomaterials would facilitate reuse.
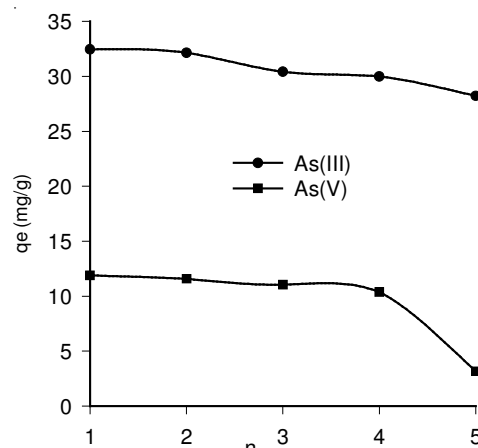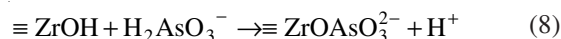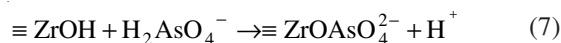

Fig. 8. Adsorption capacity of original and the regenerate adsorbent. pH = 7; adsorbent: 1 mg/mL; temperature: 25 °C; initial As(III/V) concentration: 50 mg/L

Removal efficiency of As(III/V) solution: All of the sorbents are used for removal of As(III) and As(V) from solution so does $Fe_3O_4@ZrO(OH)_2$. It is necessary to research the removal efficiency of As(III/V) solution by $Fe_3O_4@ZrO(OH)_2$. The experiment was carried out with 10 mg/L of As(III) and 1 mg/L of As(V) solution on $Fe_3O_4@ZrO(OH)_2$(10:3) adsorbents which mass more and more. The As(III/V) concentration of solution were reduced less than 10 ppb. Removal efficiency exceeds 99.9 % (Fig. 9).

Adsorption behaviour and possible mechanism: ZrO$(OH)_2$ is usually considered as the base for gel polymer formations of zirconium oxyhydrate[29]. The constitutional formula of arsenous acid [As(III)] and arsenic acid [As(V)] was also provided (Fig. 10). The zirconium atom appears two hydroxyl groups and one oxygroup. The arsenous acid atom links three hydroxyl groups and the arsenic acid atom connects two hydroxyl groups and one oxygroup.

The probable response equations[30,31], which could describe the adsorption mechanism of As(III) and As(V), were adsorbed by $Fe_3O_4@ZrO(OH)$.

$$\equiv ZrOH + H_2AsO_4^- \rightarrow\ \equiv ZrOAsO_4^{2-} + H^+ \qquad (7)$$

$$\equiv ZrOH + H_2AsO_3^- \rightarrow\ \equiv ZrOAsO_3^{2-} + H^+ \qquad (8)$$

Both arsenate and arsenite would adsorb to $Fe_3O_4@ZrO(OH)_2$ by a ligand exchange reaction. That is -OH from zirconium oxyhydrate and $-H_2AsO_4^-/-H_2AsO_3^-$ from As(V/III) by ligand exchange reaction.

The former phenomenon can be easily explained. The three-dimensional space structure of As(III) and As(V) are
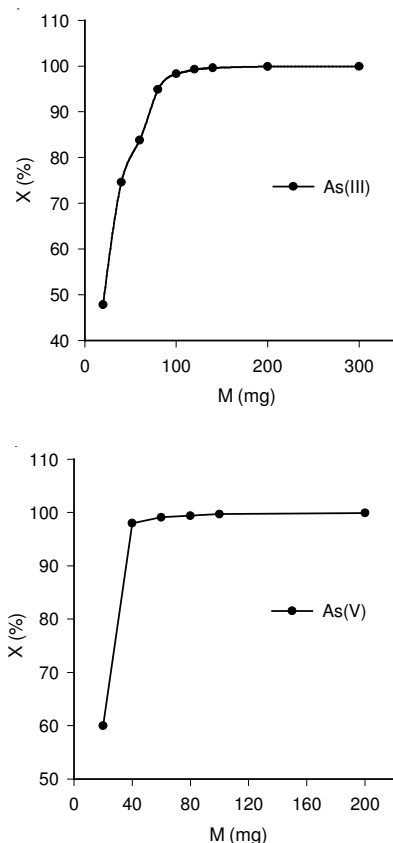
Fig. 9.   Effects of adsorbent dosage on As(III/V) removal using adsorbent. pH = 7; adsorbent: 1 mg/mL; temperature: 25 ℃; initial As(III/V) concentration: (10/1) mg/L
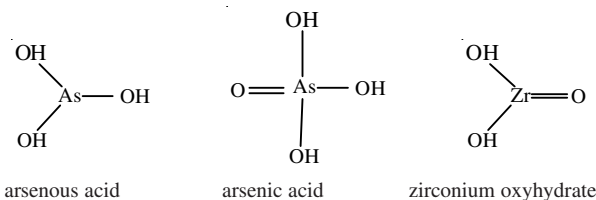

Fig. 10. Structure of the arsenous acid, arsenic acid and zirconium oxyhydrate

plane triangle and tetrahedron, respectively. It is well known that the little steric hinderance will make adsorption easier. However, the steric hinderance of tetrahedron is larger than plane triangle. So the magnetic $Fe_3O_4@ZrO(OH)_2$ adsorbents possess high adsorption capacity of As(III) than As(V). Meanwhile, why As(V) can reach to adsorption equilibrium faster than As(III) also may be understood.

As(III) and As(V) in different pH waters have their different forms. The monovalent anionic species of arsenate ($H_2AsO_4^-$) is predominant at pH 2-6, while that of arsenite ($H_2AsO_3^-$) range from 9-12[32]. According to the eqns. 7 and 8, an oxyhydrate with a negative charge in the zirconium oxyhydrate react with $H_2AsO_4^-$ and $H_2AsO_3^-$ in proportion of 1:1, while other forms of the arsenate or the arsenite is larger than $H_2AsO_4^-$ or $H_2AsO_3^-$. So the same amount of oxyhydrate easier reacts with monovalent anions more than multivalent anions.

We can explain why the optimal pH ranged from 2-6 for $H_2AsO_4^-$ while 9-12 for $H_2AsO_3^-$. But at high pH, existing desorption effect adsorption capacity about As(III).

Characterization of $Fe_3O_4@ZrO(OH)_2$ adsorbents: The TEM image (Fig. 11) of $Fe_3O_4@ZrO(OH)_2$ nanoparticles clearly reveals the spherical surface feature, which endows the same particle size. The diameter of the particles was in between 10-15 nm.
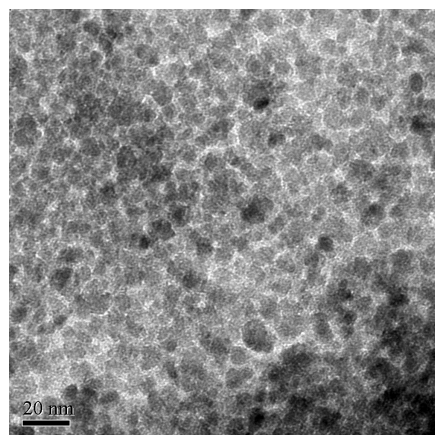

Fig. 11. TEM figure of the $Fe_3O_4@ZrO(OH)_2$

The XRD patterns of pure $ZrO(OH)_2$, Fe_3O_4 and $Fe_3O_4@ZrO(OH)_2$ nanoparticles were described in Fig. 12. It clearly shown the $ZrO(OH)_2$ has not appear, Fe_3O_4 has more apparent characteristic peak appeared. The $Fe_3O_4@ZrO(OH)_2$ has the similar characteristic peak with Fe_3O_4, but its strength decrease obviously. So it will be concluded the $Fe_3O_4@ZrO(OH)_2$ retained some characteristics of Fe_3O_4, while it may contain other substances in its surface. The VSM magnetization curves of Fe_3O_4 nanoparticles, $Fe_3O_4@ZrO(OH)_2$ nanoparticles at room temperature was shown in Fig. 13. It can be known the magnetic nanoparticles exhibited typical magnetic behaviour, characterized with strong magnetic susceptibility, is a key factor for successful magnetic separation. Due to the weight contribution from the nonmagnetic $ZrO(OH)_2$, $ZrO(OH)_2$ amount increase results in the adsorbents magnetic strength decline.

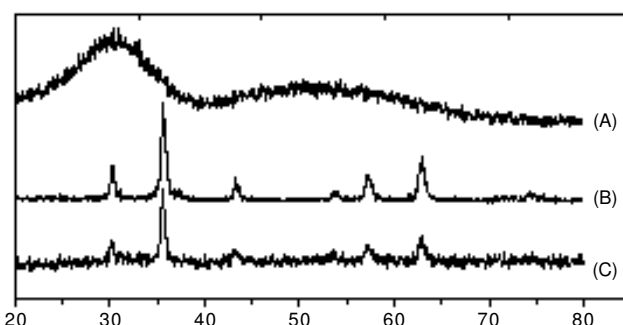Fig. 12. XRD map comparison of the $ZrO(OH)_2$(A), Fe_3O_4(B) and $Fe_3O_4@ZrO(OH)_2$(C)

Conclusion

This work investigated the synthesized method of magnetic nanoparticles $Fe_3O_4@ZrO(OH)_2$ and the adsorption property removal of As(III/V) solution. The $Fe_3O_4@ZrO(OH)_2$ puts up these attractive merits: (a) High adsorption capacity toward As(III/V), especially to As(III) than others traditionnel
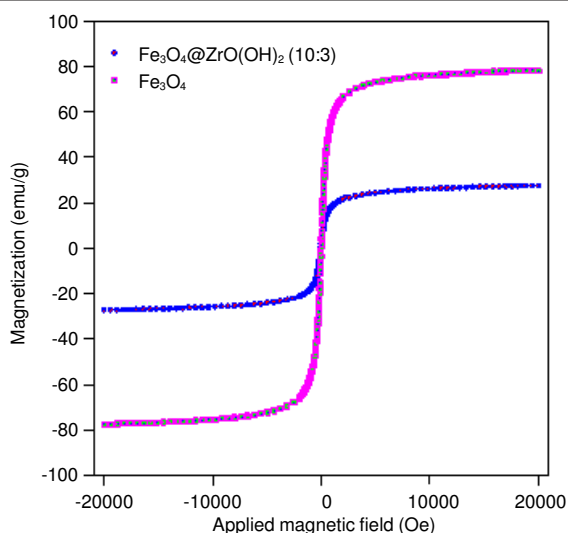
Fig. 13. VSM map comparison of the Fe₃O₄@ZrO(OH)₂ and Fe₃O₄

adsorbents owing to higher surface areas and zirconium possess natural affinity to arsenic. (b) Facile desorption, which can extend its adsorption times, meanwhile,its adsorption capacity not to decrease. (c) Rapid treatment effect, the Fe₃O₄@ZrO(OH)₂ can reduce time of reaction equilibrium concentration. In addition ferromagnetism can reduce time of solid-liquid separation by applied magnetic field. (d) Easy preparation, materials and implements of composing Fe₃O₄@ZrO(OH)₂ are business to buy. These merits have the very good application prospects.

ACKNOWLEDGEMENTS

REFERENCES

1. H.M. Anawar, J. Akai, K.M.G. Mostofa, S. Safiullah and S.M. Tareq, *Environ. Int*., **27**, 597 (2002).
2. C.A. Martinson and K.J. Reddy, *J. Colloid Interf. Sci*., **336**, 406 (2009).
3. W.J. Shao, X.M. Li, Q.L. Cao, F. Luo, J.M. Li and Y.Y. Du, *Hydrometallurgy*, **91**, 138 (2008).
4. C.M. Steinmaus, Y. Yuan and A.H. Smith, *Environ. Res*., **99**, 164 (2005).
5. M.H. Stanic, B. Kalajdzic, M. Kuleš and N. Velic, *Desalination*, **229**, 1 (2008).
6. M.B. Baskan and A. Pala, *J. Hazard. Mater*., **166**, 796 (2009).
7. B. Han, T. Runnells, J. Zimbron and R. Wickramasinghe, *Desalination*, **145**, 293 (2002).
8. F.G.A. Vagliasindi and M.M. Benjamin, *Water Sci. Technol*., **38**, 337 (1998).
9. S.B. Rasul, A.K.M. Munir, Z.A. Hossain, A.H. Khan, M. Alauddin and A. Hussam, *Talanta*, **58**, 33 (2002).
10. P.K. Pandey, S. Choubey, Y. Verma, M. Pandey and K. Chandrashekhar, *Bioresour. Technol*., **100**, 634 (2009).
11. D. Qu, J.Wang, D. Hou, Z. Luan, B. Fan and C. Zhao, *J. Hazard. Mater*., **163**, 874 (2009).
12. A. Ramaswami, S. Tawachsupa and M. Isleyen, *Water Res*., **35**, 4474 (2001).
13. O.S. Thirunavukkarasu, T. Viraraghavan and K.S. Subramanian, *Water Air Soil Pollut*., **142**, 95 (2003).
14. A. Jain and R.H. Loeppert, *J. Environ. Qual*., **29**, 1422 (2000).
15. H.W. Sun, L. Wang and R.H. Zhang, *J. Hazard. Mater*., **129**, 297 (2006).
16. J.G. Parsons, M.L. Lopez, J.R. Peralta-Videa and J.L. Gardea-Torresdey, *Microchem. J*., **91**, 100 (2009).
17. Y.F. Jia, L.Y. Xu, Z. Fang and G.P. Demopoulos, *Environ. Sci. Technol*., **40**, 3248 (2006).
18. D.W. Oscarson, P.M. Huang, U.T. Hammer and W.K. Liaw, *Water, Air, Soil Pollut*., **20**, 233 (1983).
19. Y.R. Li, J. Wang, Z.K. Luan and Z. Liang, *J. Hazard. Mater*., **177**, 131 (2010).
20. N. Haque, G. Morrison, I. Cano-Aguilera and J.L. Gardea-Torresdey, *Microchem. J*., **88**, 7 (2008).
21. V.K. Gupta, V.K. Saini and N. Jain, *J. Colloid Interf. Sci*., **288**, 55 (2005).
22. H.S. Altundogan, S. Altundogan, F. Tumen and M. Bildik, *Waste Manage*., **22**, 357 (2002).
23. K. Gupta and U.C. Ghosh, *J. Hazard. Mater*., **161**, 884 (2009).
24. X.L. Zhao, J.M. Wang, F.C. Wu, T. Wang, Y.Q. Cai, Y.L. Shi and G.B. Jiang, *J. Hazard. Mater*., **173**, 102 (2010).
25. F.E. Hadri, A.M. Rubio and M. de la Guardia, *Talanta*, **52**, 653 (2000).
26. H. Uslu, *Chem. Eng. J*., **155**, 320 (2009).
27. O. Sracek, P. Bhattacharya and G. Jacks, *Appl. Geochem*., **19**, 169 (2004).
28. S. Sarkar, L.M. Blaney, A. Gupta, D. Ghosh and A.K. SenGupta, *Environ. Sci. Technol*., **42**, 4268 (2008).
29. K.N. Ghimire, K. Inoue, H. Yamaguchi, K. Makino and T. Miyajima, *Water Res*., **37**, 4945 (2003).
30. T. Balaji, T. Yokoyama and H. Matsunaga, *Chemosphere*, **59**, 1169 (2005).
31. G.T. Schmidt, N. Vlasova, D. Zuzaan, M. Kersten and B. Daus, *J. Colloid Interf. Sci*., **317**, 228 (2008).
32. A.J. Bard, R. Parsons and J. Jordan, Marcel Dekker, New York, p. 162 (1985).